JOURNAL OF AGRICULTURAL AND FOOD CHEMISTRY

Article

pubs.acs.org/JAFC

Synthesis, Crystal Structure, in Vitro Acetohydroxyacid Synthase Inhibition, in Vivo Herbicidal Activity, and 3D-QSAR of New Asymmetric Aryl Disulfides

Jun Shang, Wei-Min Wang, Yong-Hong Li, Hai-Bin Song, Zheng-Ming Li, and Jian-Guo Wang*

State Key Laboratory and Institute of Elemento-Organic Chemistry, Nankai University, Tianjin 300071, China

Supporting Information

ABSTRACT: Acetohydroxyacid synthase (AHAS; EC 2.2.1.6) is an important bioactive target for the design of environmentally benign herbicides. On the basis of previous virtual screening, 50 asymmetric aryl disulfides containing [1,2,4]triazole groups were synthesized and characterized by ^{1}H NMR, HRMS, and crystal structure. Compounds **I-a**, **I-b**, and **I-p** show K_i values of 1.70, 4.69, and 5.57 μM, respectively, for wild type *Arabidopsis thaliana* AHAS (*At*AHAS) and low resistance against mutant type *At*AHAS W574L. At 100 mg L^{-1} concentration, compounds **I-a**, **II-a**, and **II-b** exhibit 86.6, 81.7, and 87.5% in vivo rape root growth inhibition. CoMFA steric and electrostatic contour maps were established, and a possible binding mode was suggested from molecular docking, which provide valuable information to understand the key structural features of these disulfide compounds. To the authors' knowledge, this is the first comprehensive case suggesting that asymmetric aryl disulfides are novel AHAS inhibitors.

KEYWORDS: *AHAS, molecular design, branched-chain amino acids, chemical synthesis, asymmetric aryl disulfides, crystal structure, biological activity, herbicide, molecular docking, 3D-QSAR*

INTRODUCTION

The branched-chain amino acids (BCAAs) biosynthetic pathway exists only in plants and micro-organisms, not in the bodies of mammals. For this reason, enzymes involved in the BCAAs biosynthesis pathway are ideal targets for the design of environmentally benign "green" herbicides.[1] Acetohydroxyacid synthase (AHAS; EC 2.2.1.6, also referred to as acetolactate synthase, ALS) is the first enzyme in this biological event and has been a successful herbicide target since the 1980s.[2−4] Mainly there are four families of commercial herbicidal AHAS inhibitors: sulfonylureas, imidazolinones, pyrimidinylthio (or oxo) benzoates, and triazolopyrimidine sulfonanilides.[5,6]

It was not until the 2000s that the mode of action of AHAS inhibitors became clear, when crystal structures of yeast AHAS and plant AHAS in complex with commercial herbicides were continuously determined by Guddat et al.[7−12] These studies not only have added to the understanding of the catalysis and inhibition mechanism of AHAS[13−15] or helped to interpret the relationship of the enzyme residue mutations and herbicide resistance[16] but also have provided excellent models to rationally design novel inhibitors.[17−20]

In 2007, we virtually screened the ACD-3D database and successfully identified some novel plant AHAS inhibitors.[21] Among the hits, a disulfide structure (Figure 1A) that shows strong inhibition against *Arabidopsis thaliana* AHAS (*At*AHAS) attracted us. It is a coincidence that Yoon et al. carried out high-throughput screening, and some disulfide compounds (Figure 1B) were also discovered to show potent inhibition against *Mycobacterium tuberculosis* AHAS and *Haemophilus influenzae* AHAS.[22,23] Here, we have designed and synthesized a series of asymmetric aryl disulfides containing [1,2,4]triazole groups to test their inhibition of plant AHAS and to see if these compounds possess herbicidal activity.

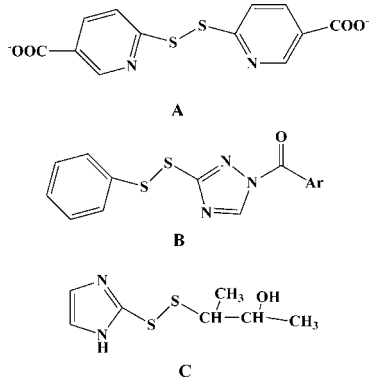

Figure 1. Some reported disulfides as AHAS inhibitors (A, B) or anticancer agents (C).

Disulfide bonds play essential roles for bioactive proteins to keep their correct folding.[24] There are a few examples that simple disulfide compounds such as diallyl disulfide and dimethyl disulfide exhibit hypochlorous acid scavenging activity[25] and tyrosinase inhibitory activity.[26] Some imidazolyl disulfides (Figure 1C) were reported to display anticancer activity.[27] However, there are no reports that disulfides have herbicidal activity. This paper describes the first study on the in vitro and in vivo activities of asymmetric aryl disulfides as plant

Received: May 21, 2012
Revised: July 27, 2012
Accepted: July 31, 2012
Published: August 20, 2012

AHAS inhibitors. These disulfides are also potent inhibitors of some resistant types of plant AHAS. The −S−S− bond was observed in the crystal structure of the typical compound. Computational three-dimensional quantitative structure−activity relationship (3D-QSAR) analysis and molecular docking were also undertaken, which provided valuable information to understand the possible binding mode and to design more potent inhibitors.

MATERIALS AND METHODS

General Synthesis and Instruments. The starting chemical materials were purchased from Tianjin Guangfu Fine Chemical Research Institute, Alfa-Aesar, or Shanghai Aladdin Regeants. All solvents and liquid reagents were dried by standard methods in advance and distilled before use. Melting points were determined using an X-4 melting apparatus (Beijing Tech Instruments Co., Beijing, China) and were uncorrected. ^{1}H NMR spectra were obtained using a 400 MHz Varian Mercury Plus 400 spectrometer in DMSO-d_6 with TMS as an internal standard. HRMS data were obtained on an FTICR-MS instrument (Ionspec 7.0T). The control herbicide monosulfuron ester was synthesized in our laboratory.[28] Molecular modeling studies were performed using an SGI 350 server.

Procedures for the Synthesis of the Target Compounds I, II, and III (Scheme 1). Example Compound I-a. The commercial

Scheme 1. Synthetic Route of the Asymmetric Aryl Disulfide Compounds

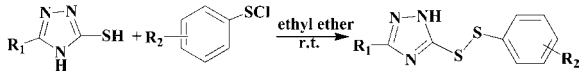

sources or the synthesis procedure of substituted [1,2,4]triazole-3-thiol (A) and arenesulfenyl chloride (B) are described in the Supporting Information. The synthesis route of the target compounds is shown in Scheme 1. For the synthesis of compound **I-a**, [1,2,4]triazole-3-thiol (0.50 g, 5 mmol) was added to a solution of freshly prepared phenylsulfenyl chlorine **a** (0.72 g, 5 mmol) in 15 mL of anhydrous ethyl ether at room temperature. The reaction mixture was stirred for 5 h at the same temperature to give a white precipitate. The product was filtered, washed with anhydrous ethyl ether, and further purified by silica gel column chromatography, when pure **I-a** was obtained: yield, 94%; mp, 85−87 °C; ^{1}H NMR (DMSO-d_6, 400 MHz) δ 8.61 (s, 1H, NHCH), 7.67 (d, J = 7.2 Hz, 2H, ArH), 7.41 (t, J = 7.4 Hz, 2H, ArH), 7.34 (d, J = 7.1 Hz, 1H, ArH); HRMS (ESI), m/z $[M + H]^+$ calcd for $C_8H_7N_3S_2$ 210.0154, found 210.0152. The same method was used to synthesize and purify compounds **I-b**−**I-v**, **II-a**−**II-n**, and **III-a**−**III-n**.

Analytical data for compounds **I-b**−**I-v**, **II-a**−**II-n**, and **III-a**−**III-n** are detailed in the Supporting Information.

X-ray Diffraction. The crystal structure of compound **I-a** (0.20 × 0.18 × 0.10 mm in size) was determined, and X-ray intensity data were recorded on a Rigaku Saturn 724 CCD diffraction meter using graphite monochromated Mo KR radiation (λ = 0.71073 Å). The Bruker software package *SHELXTL* was used to solve the structure using "direct methods" techniques.[29] All calculations were refined anisotropically.

Biological Assays. *Determination of Inhibition of Arabidopsis thaliana AHAS (AtAHAS).* The expression and purification of wild type *At*AHAS and mutant type *At*AHAS W574L have been described previously.[30] AHAS activity was measured using the colorimetric assay in a previous publication, and K_i values were estimated using the following equation, where v_0 is the uninhibited rate:[31]

$$v = v_0/(1 + [I]/K_i)$$

In Vivo Inhibition of the Root Growth of Rape (Brassica campestris L.). The in vivo rape root growth inhibition data were determined using the previously published method.[31]

Molecular Modeling. *Comparative Molecular Field Analysis (CoMFA) Analysis.* The chemical structures of the compounds were built within Sybyl 7.3 (Tripos Inc., St. Louis, MO, USA) based on the crystal structure of compound **I-a**. All of the molecules were assigned Gasteiger−Hückel charges and minimized by the Tripos force field when convergence reached 0.001 kcal mol^{-1} Å^{-1}. **I-a** was used as the template to superimpose all of the disulfides. CoMFA was used for the 3D-QSAR analysis.[32] The cutoff was set to 30 kcal mol^{-1}, and column filtering was set to 2.0 kcal mol^{-1}; all other default values in the setting were used. The "leave-one-out" (LOO) cross-validation method was applied to determine the optimum number of partial least-squares (PLS) components. The biological activities were expressed in terms of D using the following formula that has been explained elsewhere:[33]

$$D = \log_{10}[a/(1 - a)] + \log_{10} M_w$$

Molecular Docking. The molecular docking of the disulfides to *At*AHAS was performed by FlexX.[34] The docking method is similar to our published procedure, and all default values were used for the molecular simulation.[21] Compounds that have in vitro *At*AHAS percent inhibition >70% at 10 mg L^{-1} concentration were docked to the *At*AHAS binding site. The dominant conformations of the docked molecules were chosen for further analysis. The figures were generated by Sybyl 7.3 and LIGPLOT.[35]

RESULTS AND DISCUSSION

Synthetic Chemistry of the Target Compounds. All of the target compounds were characterized by ^{1}H NMR and HRMS. Their molecular structures are listed in Table 1.

Our synthetic work dated back to early 2010. In 2011, we noticed that Hahn et al. reported a novel method that asymmetric disulfides can be prepared in a reaction similar to ours.[36] In that case, moist tetrahydrofuran gave better yields than dried benzene as the solvent for the reaction, so the authors added 5−10 M equivalent of water to the reaction mixture and observed satisfactory yields. Thus, the presence of water was thought to be preferable for the reaction. However, it is surprising that these researchers did not notice an important patent, which in 1983 reported that the reaction of sulfenyl chloride with thiols can occur easily using various ethers as the solvent.[37] Here, we have synthesized 50 asymmetric aryl disulfides (compounds **I-a** and **I-g** were previously coincidently reported by Hahn et al. in the literature [36]) using only ethyl ether as solvent under very mild conditions, and most of the yields for the reactions are >90%. Compared with Hahn's method, our synthetic method is more straightforward. Our results indicate that this type of reaction does not require additional water as essential reactant or catalyst to afford high yield.

Crystal Structure Analysis. Compound **I-a** was recrystallized from ethanol/dichloromethane to give colorless crystals suitable for X-ray single-crystal diffraction. In the range of 2.91° ≤ θ ≤ 27.89°, 2197 independent reflections were obtained. The compound crystallized in the orthorhombic system, and the space group is $P2_12_12_1$. The crystallographic parameters are as follows: a = 9.412(5) Å, b = 9.813(5) Å, c = 9.964(5) Å, α = 90°, β = 90°, γ = 90°, μ = 0.530 mm^{-1}, V = 0.9202(9) nm^3, Z = 4, D_c = 1.511 g cm^{-3}, $F(000)$ = 432. The final R factors are R_1 = 0.0259 and ωR_2 = 0.0518.

The crystal structure of **I-a** is shown in Figure 2. The linkage of the −S−S− bond between the phenyl ring and the triazole ring can be seen. The whole molecule adopts a twist shape. The bond lengths in the phenyl ring are similar, whereas in the heterocycle, bonds C(2)−N(3), N(1)−C(1), and C(1)−N(2) are shorter than bonds N(1)−C(2) and N(2)−N(3). It is notable that the N(2) atom is attached with a hydrogen atom. The dihedral angle between the triazole ring and the phenyl

dx.doi.org/10.1021/jf302206x | J. Agric. Food Chem. 2012, 60, 8286−8293

Table 1. Chemical Structures of the Target Asymmetric Disulfides

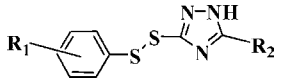

No.	R_1	R_2	No.	R_1	R_2
I-a	H	H	II-d	2-$COOC_2H_5$	
I-b	4-CH_3	H	II-e	2-NO_2	
I-c	2-$COOCH_3$	H	II-f	4-OCH_3	
I-d	2-$COOC_2H_5$	H	II-g	4-Cl	
I-e	2-NO_2	H	II-h	H	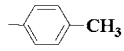
I-f	4-OCH_3	H	II-i	4-CH_3	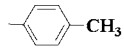
I-g	4-Cl	H	II-j	2-$COOCH_3$	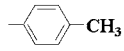
I-h	4-Br	H	II-k	2-$COOC_2H_5$	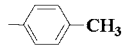
I-i	2-F	H	II-l	2-NO_2	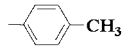
I-j	2-CH_3	H	II-m	4-OCH_3	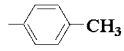
I-k	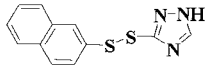		II-n	4-Cl	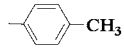
I-l	H	CH_3	III-a	H	
I-m	4-CH_3	CH_3	III-b	4-CH_3	
I-n	2-$COOCH_3$	CH_3	III-c	2-$COOCH_3$	
I-o	2-$COOC_2H_5$	CH_3	III-d	2-$COOC_2H_5$	
I-p	2-NO_2	CH_3	III-e	2-NO_2	
I-q	4-OCH_3	CH_3	III-f	4-OCH_3	
I-r	4-Cl	CH_3	III-g	4-Cl	
I-s	4-Br	CH_3	III-h	H	
I-t	2-F	CH_3	III-i	4-CH_3	
I-u	2-CH_3	CH_3	III-j	2-$COOCH_3$	
I-v	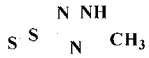		III-k	2-$COOC_2H_5$	
II-a	H		III-l	2-NO_2	
II-b	4-CH_3		III-m	4-OCH_3	
II-c	2-$COOCH_3$		III-n	4-Cl	

ring is 63.5°. The selected bond lengths and torsion angles are listed in the Supporting Information.

Biological Activity. The in vitro wild type *At*AHAS inhibition and in vivo herbicidal activity of the 50 asymmetric aryl disulfides are listed in Table 2. The in vitro activity was evaluated at 100, 10, 3, and 1 mg L^{-1} concentrations. The in vivo herbicidal activity was measured using the rape root growth inhibition method at 100 mg L^{-1} concentration. A commercialized

dx.doi.org/10.1021/jf302206x | J. Agric. Food Chem. 2012, 60, 8286−8293

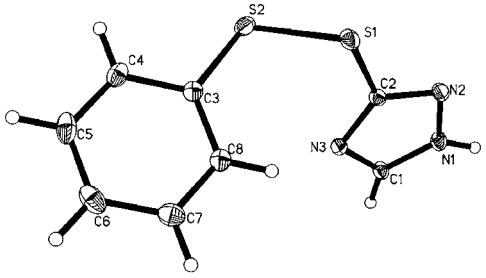

Figure 2. Molecular structure of compound **I-a**.

sulfonylurea herbicide, monosulfuron ester, was used as a control.

For the in vitro biological activities, most of the compounds exhibited desirable inhibition against wild type *At*AHAS at 100 mg L^{-1} concentration, and nearly half of the compounds have percent inhibition >80%. It is encouraging that at a low concentration of 3 mg L^{-1}, compounds **I-a**, **I-b**, **I-c**, **I-d**, **I-e**, **I-f**, **I-k**, **I-n**, **I-p**, **I-r**, **I-s**, and **I-t** still have inhibition >60%. The inhibition constants of compounds **I-a**, **I-b**, and **I-p** are 1.70 ± 0.08, 4.69 ± 0.39, and 5.57 ± 0.61 μM (Table 3), which are similar to the K_i values of imidazolinone herbicides (ranging from 3 to 16 μM),[30] but not as good as those of sulfonylurea herbicides (ranging from 8 to 400 nM).[30,31] The inhibition curve of representative compound **I-a** is shown in Figure 3. On the basis of the preliminary in vitro AHAS inhibition data, the asymmetric disulfides appear to be promising new plant AHAS inhibitors.

When subjected to W574L inhibition assay, compounds **I-a**, **I-b**, and **I-p** still have K_i values of 24.5 ± 2.4, 25.7 ± 5.3, and 27.1 ± 5.5 μM, respectively (Table 3). Similar to the definition from a previous publication,[30] resistance here means the ratio of K_i for W574L compared with that of the wild type *At*AHAS for the same inhibitor. In this study, resistance data for **I-a**, **I-b**, and **I-p** are 14.4, 5.5 and 4.9, which are low resistance levels. However, for the same mutant type, K_i values are 85.3 ± 19.2 μM (data in this study) for monosulfuron ester and 470 ± 2 μM for imazaquin (data from the literature[30]). The corresponding resistance values for monosulfuron ester and imazaquin against W574L are 320 and 161, much higher than those of compound **I-a**, **I-b**, and **I-p**. Usually, for W574L, the sulfonylureas cover a resistance range of 130−2830 and the imidazolinones have a resistance range of 155−186.[30] As summarized by Duggleby et al. in 2008,[38] W574L mutation even leads to strong resistance for pyrimidinylthio (or oxo) benzoates and triazolopyrimidine sulfonanilides for cocklebur AHAS (corresponding residue number W552L). It is exciting that the current disulfide compounds have obvious advantages over the sulfonyluea and imidazolinone herbicides against W574L. This result will attract our interest to further investigate the molecular basis of asymmetric aryl disulfides as novel AHAS inhibitors.

The target compounds also displayed significant in vivo rape root growth inhibition at 100 mg L^{-1} concentration. The herbicidal activities for **I-a**, **II-a**, and **II-b** are 86.6, 81.7, and 87.5%, similar to the level of monosulfuron ester, which has an inhibition of 88.5%. Moreover, compounds **I-b**, **I-c**, **I-e**, **I-g**, **I-l**, **I-m**, **I-p**, **II-c**, **II-h**, **III-a**, and **III-h** showed >50% rape root growth inhibition at the test condition. Thus, the asymmetric disulfides not only exhibit strong in vitro AHAS inhibition but also show good herbicidal activity. It should be noted that for **I-a**, **I-b**, **I-c**, **I-e**, **I-l**, **I-m**, **I-p**, **II-h**, **III-a**, and **III-h**, the wild type *At*AHAS inhibition data at 100 mg L^{-1} are all >95% and the inhibition data at 10 mg L^{-1} are all >80%. This indicates that these compounds may undergo some loss after the absorption, distribution, metabolism, and excretion (ADME) process.

Table 2. In Vitro AtAHAS Inhibition and in Vivo Herbicidal Activity of the Asymmetric Aryl Disulfides

	*At*AHAS inhibition (%)				rape root growth inhibition (%)
compd	100 mg L^{-1}	10 mg L^{-1}	3 mg L^{-1}	1 mg L^{-1}	100 mg L^{-1}
I-a	97	91	79	50	86.6
I-b	96	86	70	48	67.5
I-c	97	86	81	39	54.8
I-d	94	87	80	44	21.1
I-e	96	87	81	36	69.8
I-f	90	75	63	3	44.6
I-g	48	0	0	0	50.2
I-h	43	0	0	0	27.4
I-i	84	70	59	7	47.2
I-j	93	80	59	3	43.6
I-k	91	76	65	19	16.3
I-l	96	86	54	0	69.4
I-m	97	84	47	0	62.5
I-n	92	80	63	46	10.6
I-o	83	69	17	0	26.6
I-p	95	81	76	48	59.6
I-q	80	66	56	11	28.3
I-r	86	66	60	26	24.1
I-s	84	67	61	15	17.6
I-t	85	72	60	11	13
I-u	43	0	0	0	36.8
I-v	87	79	52	19	0
II-a	82	66	54	0	81.7
II-b	69	58	0	0	87.5
II-c	62	43	0	0	52.8
II-d	61	39	0	0	34.3
II-e	74	52	0	0	0
II-f	84	18	0	0	29.4
II-g	57	0	0	0	37.5
II-h	94	83	16	0	54.1
II-i	55	15	0	0	0
II-j	48	0	0	0	44.9
II-k	29	15	0	0	0
II-l	52	37	0	0	0
II-m	74	6	0	0	11
II-n	56	0	0	0	24.1
III-a	96	86	34	0	70.2
III-b	48	30	0	0	6.9
III-c	81	60	12	0	30.5
III-d	60	49	28	0	0
III-e	86	72	16	0	0
III-f	69	0	0	0	0
III-g	78	54	13	0	0
III-h	97	92	54	9	66.2
III-i	48	26	0	0	0
III-j	87	70	40	0	0
III-k	55	30	0	0	0
III-l	61	38	31	0	27.4
III-m	80	53	20	0	14.3
III-n	85	65	29	0	0
monosulfuron ester	98	95	92	85	88.5

dx.doi.org/10.1021/jf302206x | *J. Agric. Food Chem.* 2012, 60, 8286−8293

Table 3. K_i Values of Representative Disulfides against Wild Type *At*AHAS and Mutant Type *At*AHAS W547L

compd	K_i (μM) for *At*AHAS wild type	K_i (μM) for *At*AHAS W574L	resistance
I-a	1.70 ± 0.08	24.5 ± 2.4	14.4
I-b	4.69 ± 0.39	25.7 ± 5.3	5.5
I-p	5.57 ± 0.61	27.1 ± 5.5	4.9
monosulfuron ester	0.26 ± 0.03	8.53 ± 1.92	320
imazaquin[a]	3.0 ± 0.1	470 ± 20	161

[a]Data from the literature.[30]

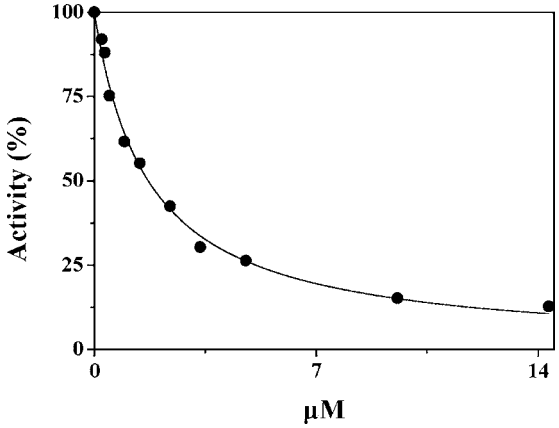

Figure 3. Inhibition curve of compound **I-a** against wild type *At*AHAS.

However, for **I-g**, **II-a**, **II-b**, and **II-c**, their in vivo biological activities at 100 mg L^{-1} show a good correlation with the in vitro inhibition data, despite the fact that their in vitro inhibition data at 100 mg L^{-1} are <85% and at 10 mg L^{-1} are <66%, meaning that these compounds may have high efficiency to bind with the plant AHAS for in vivo herbicidal assay. Bearing these facts in mind, compounds with enhanced herbicidal activity can be further designed and evaluated.

Quantitative Structure–Activity Relationships. The alignment of the compounds is shown in the Supporting Information. The biological activity *D* values were calculated on the basis of the in vitro data at 10 mg L^{-1} concentration. Compounds **I-g**, **I-h**, **I-u**, **II-g**, **II-j**, **II-n**, and **III-f** were excluded because their inhibition values are 0. For the CoMFA computation, compound **I-m** was also removed from the training set as an outlier. The leave-one-out q^2 value is 0.603 when the optimum number of components is 7, indicating that the model is reliable. The non-cross-validated r^2 value is 0.903, with a standard error of estimate of 0.17 and an *F* value of 45.195. The steric and electrostatic contributions are 61.6 and 38.4%, respectively. The predictive biological activity versus the experimental biological activity are plotted in the Supporting Information.

The 3D-CoMFA contour maps are shown in Figure 4. Compound **I-a** was used as the template to illustrate the structure–activity relationships. For the electrostatic contour map (Figure 4A), the blue contour defines a region where an increase in the positive charge will result in an increase of activity, whereas the red contour defines a region of space where negative charge is favorable. It can be observed that the electrostatically favored region locates at *ortho*- or *meta*-positions of the phenyl ring, whereas the electrostatically disfavored region covered a large space around the phenyl ring. For the steric contour map (Figure 4B), the green part displays

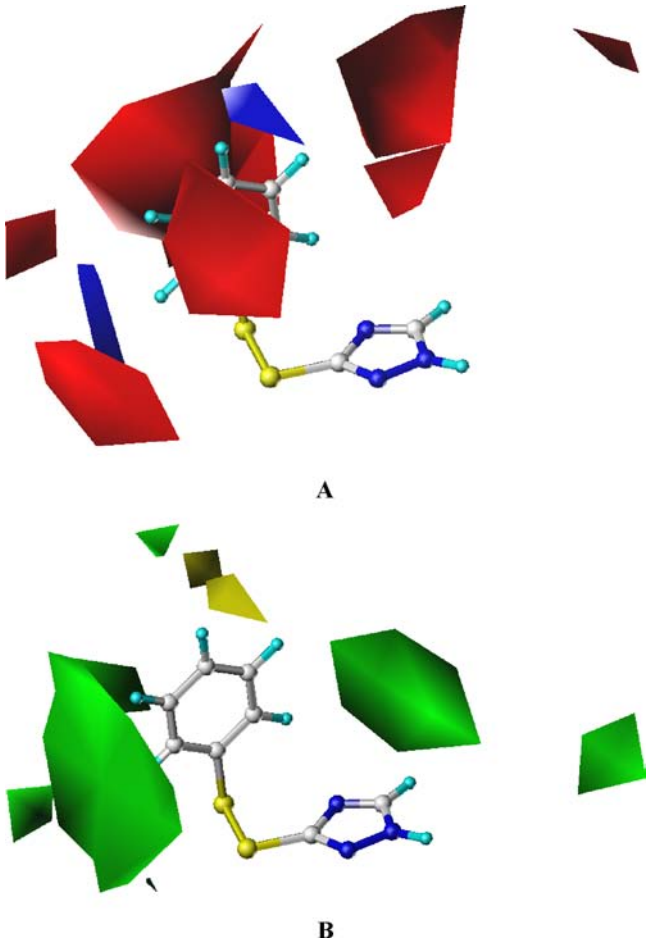

Figure 4. Electrostatic contour map (A) and steric contour map (B) for the CoMFA model. In map A, positive charge favored regions are shown in blue and negative charge favored regions are shown in red. In map B, sterically favored regions are shown in green and sterically disfavored regions are shown in yellow.

a position where a bulky group would be favorable for potent inhibition and the yellow part represents a position where a bulky group is likely to decrease the in vitro activity. The sterically favored region covers a small space near the phenyl ring; however, the sterically disfavored space locates in bigger regions not only around the phenyl ring but also near the triazole ring. The CoMFA contour map provides valuable information for further structural optimization of this family of new AHAS inhibitors.

Molecular Docking. In total 20 compounds were docked to the herbicide binding site of *At*AHAS. After investigation of the resulting docked conformations, eight compounds (**I-a**, **I-i**, **I-j**, **I-l**, **I-t**, **II-h**, **III-a**, and **III-h**) were found to overlay one another quite well (figure in the Supporting Information). The docked conformations for the other 12 compounds (**I-b**, **I-c**, **I-d**, **I-e**, **I-f**, **I-k**, **I-m**, **I-n**, **I-p**, **I-v**, **III-e**, and **III-j**) were in unreasonable binding space, and they failed to overlay well with one another. Thus, the docked conformations of the eight compounds were regarded as the possible binding conformations in the study. Compound **I-a** was also chosen here to illustrate the binding mode of the disulfide AHAS inhibitors. Figure 5A is a two-dimensional representation of the interactions between **I-a** and surrounding residues of *At*AHAS drawn by LIGPLOT. The herbicide binding site is at the interface of two subunits. The inhibitor interacts with *At*AHAS via multiple H-bonding

dx.doi.org/10.1021/jf302206x | J. Agric. Food Chem. 2012, 60, 8286–8293

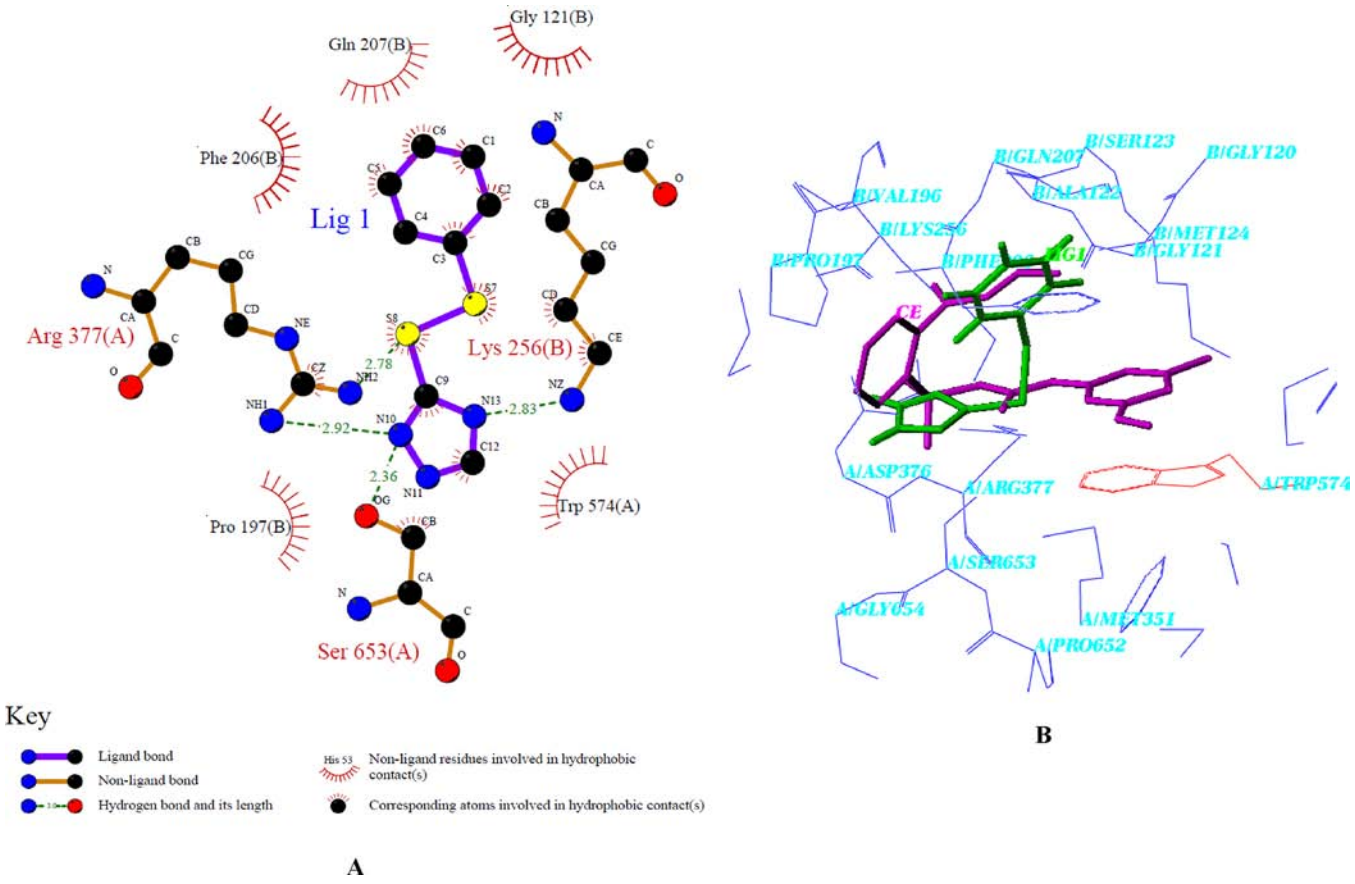

Figure 5. FlexX docking of asymmetric disulfide **I-a** to *At*AHAS. (A) 2D plot by LIGPLOT. The hydrogen bonds between the enzyme and the inhibitor are shown as green dashed lines, and distances are in Å units. Amino acid residues that are within van der Waals contact of **I-a** are shown as red arcs. An atom belonging to **I-a** that participates in van der Waals attractions to the enzyme is identified by a red star. Residues labeled with a prime are from the alternate subunit. (B) Picture drawn in Sybyl. The green molecule represents the disulfide **I-a**, the magenta molecule represents sulfonylurea herbicide chlorimuron ethyl, and the red part represents the W574 residue in *At*AHAS.

contacts and hydrophobic contacts. R377(A), S653 (A), and K256(B) form four H-bonds with the inhibitor, whereas W574(A), G121(B), P197(B), F206(B), and Q207(B) form hydrophobic interactions with the small molecule. Figure 5B is a three-dimensional picture showing the binding mode of disulfide, and it compares the modes of action between sulfonylurea chlorimuron ethyl (magenta molecule CE) and **I-a** (green molecule LIG1). It can be seen that there exists minor overlapping of the two inhibitors. However, there is significant difference between their binding modes with regard to an important residue, W574(A) (red residue). The pyrimidine ring in the sulfonylurea herbicide CE forms a strong $\pi-\pi$ stacking with the indole ring of W574, which is crucial for the tight binding of sulfonylureas with *At*AHAS. For compound **I-a**, although it makes hydrophobic contact with W574(A), there does not exist a $\pi-\pi$ stacking. This is in agreement with the W574L inhibition data, indicating that the mode of action from molecular docking is reasonable.

In summary, 50 asymmetric aryl disulfides containing [1,2,4]-triazole groups were synthesized and evaluated as novel plant AHAS inhibitors via both in vitro enzyme inhibition and in vivo rape root growth inhibition. Besides the wild type *At*AHAS, the compounds also displayed potent inhibition against mutant type *At*AHAS W574L. 3D-CoMFA contour maps were generated for design inhibitors with enhanced activity. The binding mode predicted from molecular docking reasonably explains the low resistance of the disulfides against W574L. This study indicates that asymmetric aryl disulfides should be paid more attention to discover novel herbicides to fight the resistance of current AHAS inhibitors.

■ ASSOCIATED CONTENT

Ⓢ Supporting Information

Synthesis procedure of substituted [1,2,4]triazole-3-thiol (A) and arenesulfenyl chloride (B), analytical data for compounds **I-b**−**I0v**, **II-a**−**II-n**, and **III-a**−**III-n**; selected bond lengths and torsion angles for the crystal structure of **I-a**; alignment for the training set of the CoMFA model; plot of predictive biological activity versus the experimental biological activity; and overlay of docked compounds from FlexX. This material is available free of charge via the Internet at http://pubs.acs.org.

■ AUTHOR INFORMATION

Corresponding Author

*Phone: +86-(0)22-23499414. Fax: +86-(0)22-23503627. E-mail: nkwjg@nankai.edu.cn.

Funding

We acknowledge financial support from the Natural Science Foundation of China (No. 21272128), Key Natural Science Foundation from Tianjin S&T(12JCZDJC25700), National Basic Research Project of China (No. 2010CB126103), and National Key Technology Research and Development Program (No. 2011BAE06B05-3).

Notes

The authors declare no competing financial interest.

■ ACKNOWLEDGMENTS

We appreciate associate professor Cong-Wei Niu for her kind assistance in the measurement of W754L inhibition constants of the typical disulfides.

■ REFERENCES

(1) Duggleby, R. G.; Pang, S. S. Acetohydroxyacid synthase. *J. Biochem. Mol. Biol.* **2000**, *33* (1), 1−36.

(2) Chaleff, R. S.; Mauvais, C. J. Acetolactate synthase is the site of action of two sulfonylurea herbicides in higher plants. *Science* **1984**, *224*, 1443−1445.

(3) LaRossa, R. A.; Schloss, J. V. The sulfonylurea herbicide sulfometuron methyl is an extremely potent and selective inhibitor of acetolactate synthase in *Salmonella typhimurium*. *J. Biol. Chem.* **1984**, *259*, 8753−8757.

(4) Ray, T. B. Site of action of chlorsulfuron: inhibition of valine and isoleucine biosynthesis of plants. *Plant Physiol.* **1984**, *75*, 827−831.

(5) Whitcomb, C. E. An introduction to ALS-inhibiting herbicides. *Toxicol. Ind. Health* **1999**, *15* (1−2), 231−239.

(6) McCourt, J. A.; Duggleby, R. G. Acetohydroxyacid synthase and its role in the biosynthetic pathway for branched-chain amino acids. *Amino Acids* **2006**, *31*, 173−210.

(7) Pang, S. S.; Guddat, L. W.; Duggleby, R. G. Crystallization of the catalytic subunit of *Saccharomyces cerevisiae* acetohydroxyacid synthase. *Acta Crystallogr.* **2001**, *D57*, 1321−1323.

(8) Pang, S. S.; Duggleby, R. G.; Guddat, L. W. Crystal structure of yeast acetohydroxyacid synthase: a target for herbicidal inhibitors. *J. Mol. Biol.* **2002**, *317*, 249−262.

(9) Pang, S. S.; Guddat, L. W.; Duggleby, R. G. Molecular basis of sulfonylurea herbicide inhibition of acetohydroxyacid synthase. *J. Biol. Chem.* **2003**, *278*, 7639−7644.

(10) McCourt, J. A.; Pang, S. S.; Guddat, L. W.; Duggleby, R. G. Elucidating the specificity of sulfonylurea herbicide binding to acetohydroxyacid synthase. *Biochemistry* **2005**, *44*, 2330−2338.

(11) McCourt, J. A.; Pang, S. S.; King-Scott, J.; Guddat, L. W.; Duggleby, R. G. Herbicide binding sites revealed in the structure of plant acetohydroxyacid synthase. *Proc. Natl. Acad. Sci. U.S.A.* **2006**, *103*, 569−573.

(12) Wang, J.-G.; Lee, P.; Dong, Y.-H.; Pang, S.-S.; Duggleby, R. G.; Li, Z.-M.; Guddat, L. W. Crystal structures of two novel sulfonylurea herbicides in complex with *Arabidopsis thaliana* acetohydroxyacid synthase. *FEBS J.* **2009**, *276*, 1282−1290.

(13) Xiong, Y.; Liu, J.; Yang, G. F.; Zhan, C. G. Computational determination of fundamental pathway and activation barriers for acetohydroxyacid synthase-catalyzed condensation reactions of α-keto acids. *J. Comput. Chem.* **2010**, *31* (8), 1592−1602.

(14) Duggleby, R. G.; Pang, S. S.; Yu, H.; Guddat, L. W. Systematic characterization of mutations in yeast acetohydroxyacid synthase: interpretation of herbicide-resistance data. *Eur. J. Biochem.* **2003**, *270*, 2895−2904.

(15) He, Y. Z.; Li, Y. X.; Zhu, X. L.; Xi, Z.; Niu, C.; Wan, J.; Zhang, L.; Yang, G. F. Rational design based on bioactive conformation analysis of pyrimidinylbenzoates as acetohydroxyacid synthase inhibitors by integrating molecular docking, CoMFA, CoMSIA, and DFT calculations. *J. Chem. Inf. Model.* **2007**, *47* (6), 2335−2344.

(16) Duggleby, R. G.; McCourt, J. A.; Guddat, L. W. Structure and mechanism of inhibition of plant acetohydroxyacid synthase. *Plant Physiol. Biochem.* **2008**, *46*, 309−324.

(17) Chen, C. N.; Chen, Q.; Liu, Y. C.; Zhu, X. L.; Niu, C. W.; Xi, Z.; Yang, G. F. Syntheses and herbicidal activity of new triazolopyrimidine-2-sulfonamides as acetohydroxyacid synthase inhibitor. *Bioorg. Med. Chem.* **2010**, *18* (14), 4897−4904.

(18) Chen, C. N.; Lv, L. L.; Ji, F. Q.; Chen, Q.; Xu, H.; Niu, C. W.; Xi, Z.; Yang, G. F. Design and synthesis of *N*-2,6-difluorophenyl-5-methoxyl-1,2,4-triazolo[1,5-*a*]-pyrimidine-2-sulfonamide as acetohydroxyacid synthase inhibitor. *Bioorg. Med. Chem.* **2009**, *17* (8), 3011−3017.

(19) Li, Y. X.; Luo, Y. P.; Xi, Z.; Niu, C.; He, Y. Z.; Yang, G. F. Design and syntheses of novel phthalazin-1(2*H*)-one derivatives as acetohydroxyacid synthase inhibitors. *J. Agric. Food Chem.* **2006**, *54* (24), 9135−9139.

(20) Wang, J.; Tan, H.; Li, Y.; Ma, Y.; Li, Z.; Guddat, L. W. Chemical synthesis, in vitro acetohydroxyacid synthase (AHAS) inhibition, herbicidal activity, and computational studies of isatin derivatives. *J. Agric. Food Chem.* **2011**, *59* (18), 9892−9900.

(21) Wang, J. G.; Xiao, Y. J.; Li, Y. H; Ma, Y.; Li, Z. M. Identification of some novel AHAS inhibitors via molecular docking and virtual screening approach. *Bioorg. Med. Chem.* **2007**, *15* (1), 374−380.

(22) Choi, K. J.; Yu, Y. G.; Hahn, H. G.; Choi, J. D.; Yoon, M. Y. Characterization of acetohydroxyacid synthase from *Mycobacterium tuberculosis* and the identification of its new inhibitor from the screening of a chemical library. *FEBS Lett.* **2005**, *579* (21), 4903−4310.

(23) Choi, K. J.; Noh, K. M.; Kim, D. E.; Ha, B. H.; Kim, E. E.; Yoon, M. Y. Identification of the catalytic subunit of acetohydroxyacid synthase in *Haemophilus influenzae* and its potent inhibitors. *Arch. Biochem. Biophys.* **2007**, *466* (1), 24−30.

(24) Zhang, L.; Chou, C. P.; Moo-Young, M. Disulfide bond formation and its impact on the biological activity and stability of recombinant therapeutic proteins produced by *Escherichia coli* expression system. *Biotechnol. Adv.* **2011**, *29* (6), 923−929.

(25) Argüello-García, R.; Medina-Campos, O. N.; Pérez-Hernández, N.; Pedraza-Chaverrí, J.; Ortega-Pierres, G. Hypochlorous acid scavenging activities of thioallyl compounds from garlic. *J. Agric. Food Chem.* **2010**, *58*, 11226−11233.

(26) Chu, H. L.; Wang, B. S.; Duh, P. D. Effects of selected organosulfur compounds on melanin formation. *J. Agric. Food Chem.* **2009**, *57* (15), 7072−7077.

(27) Vogt, A.; Tamura, K.; Watson, S.; Lazo, J. S. Antitumor imidazolyl disulfide IV-2 causes irreversible G(2)/M cell cycle arrest without hyperphosphorylation of cyclin-dependent kinase Cdk1. *J. Pharmacol. Exp. Ther.* **2000**, *294* (3), 1070−1075.

(28) Wang, B.-L.; Ma, N; Wang, J.-G.; Ma, Y.; Li, Z.-M.; Leng, X. B. Synthesis and dimeric crystal structure of sulfonylurea compound *N*-[2-(4-methyl)pyrimidinyl]-*N*′-2-methoxycarbonyl-benzene sulfonylurea. *Chin. J. Struct. Chem.* **2004**, *23*, 783−787.

(29) Sheldrick, G. M. A short history of *SHELX*. *Acta Crystallogr., Sect. A* **2008**, *64*, 112−122.

(30) Chang, A. K.; Duggleby, R. G. Herbicide-resistant forms of *Arabidopsis thaliana* acetohydroxyacid synthase: characterization of the catalytic properties and sensitivity to inhibitors of four defined mutants. *Biochem. J.* **1998**, *333*, 765−777.

(31) Wang, J.-G.; Li, Z.-M.; Ma, N.; Wang, B.-L.; Jiang, L.; Pang, S. S.; Lee, Y.-T.; Guddat, L. W.; Duggleby, R. G. Structure-activity relationships for a new family of sulfonylurea herbicides. *J. Comput.-Aided Mol. Des.* **2005**, *19*, 801−820.

(32) Cramer, M.; Cramer, R. D.; Jones, D. M. Comparative molecular field analysis. 1. Effect of shape on binding of steroids to carrier proteins. *J. Am. Chem. Soc.* **1988**, *110*, 5959−5967.

(33) Zhu, Y. Q.; Wu, C.; Li, H. B.; Zou, X. M.; Si, X. K.; Hu, F. Z.; Yang, H. Z. Design, synthesis, and quantitative structure-activity relationship study of herbicidal analogues of pyrazolo[5,1-*d*] [1,2,3,5]-tetrazin-4(3*H*)ones. *J. Agric. Food Chem.* **2007**, *55* (4), 1364−1369.

(34) Rarey, M.; Kramer, B.; Lengauer, T.; Klebe, G. A fast flexible docking method using an incremental construction algorithm. *J. Mol. Biol.* **1996**, *261*, 470−489.

(35) Wallace, A. C.; Laskowski, R. A.; Thornton, J. M. LIGPLOT: a program to generate schematic diagrams of protein-ligand interactions. *Protein Eng.* **1995**, *8*, 127−134.

(36) Han, M.; Lee, J. T.; Hahn, H. G. A traceless, one-pot preparation of unsymmetric disulfides from symmetric disulfides through a repeated process involving sulfenic acid and thiosulfinate intermediates. *Tetrahedron Lett.* **2011**, *52*, 236−239.

(37) Frankenthal, H. H.; Mutterstadt, H. Z.; Westheim, C. J. M.; Limburgerhof, E. H. P. *N*-Oxo-pyridin-2-yl-dithio-(4-nitro-2-tricholoromethylbenzene) and a fungicidal formulation containing same. U.S. Patent 4395415, 1981

(38) Duggleby, R. G.; McCourt, J. A.; Guddat, L. W. Structure and mechanism of inhibition of plant acetohydroxyacid synthase. *Plant Physiol. Biochem.* **2008**, *46*, 309−324.